KAPL-P-000113
(K98152)

EXTENDING THE CUTOFF WAVELENGTH OF LATTICE-MATCHED GaInAsSb/GaSb THERMOPHOTOVOLTAICS DEVICES

CONF-981055--

C. A Wang, G. W. Charache

October 1998

NOTICE

KAPL ATOMIC POWER LABORATORY SCHENECTADY, NEW YORK 12301

Operated for the U. S. Department of Energy
by KAPL, Inc. a Lockheed Martin company

DISCLAIMER

DISCLAIMER

Portions of this document may be illegible in electronic image products. Images are produced from the best available original document.

Extending the Cutoff Wavelength of Lattice-Matched GaInAsSb/GaSb Thermophotovoltaics Devices*

C.A. Wang†, H.K. Choi, D.C. Oakley
Lincoln Laboratory, Massachusetts Institute of Technology, Lexington, MA 02420-9108
G.W. Charache
Lockheed Martin, Inc., Schenectady, NY 12301

Abstract

This paper reports the growth, materials characterization, and device performance of lattice-matched GaInAsSb/GaSb thermophotovoltaic (TPV) devices with cutoff wavelength as long as 2.5 μm. GaInAsSb epilayers were grown lattice matched to GaSb substrates by organometallic vapor phase epitaxy (OMVPE) using all organometallic precursors including triethylgallium, trimethylindium, tertiarybutylarsine, and trimethylantimony with diethyltellurium and dimethylzinc as the n- and p-type dopants, respectively. The growth temperature was 525°C. Although these alloys are metastable, a mirror-like surface morphology and room temperature photoluminescence (PL) are obtained for alloys with PL peak emission at room temperature as long as 2.5 μm. In general, however, a trend of decreasing material quality is observed as the wavelength increases. Both the surface roughness and PL full width at half-maximum increase with wavelength. In spite of the dependence of material quality on PL peak emission wavelength, the internal quantum efficiency of TPV devices with cutoff wavelengths of 2.3 to 2.5 μm is as high as 86%.

Keywords: GaInAsSb, thermophotovoltaics, mid-infrared, OMVPE
PACs: 64.60.My, 68.55.Jk, 73.61.Ey, 78.55.m, 81.15.Gh, 84.60.Jt

*This work was sponsored by the Department of Energy under AF Contract No. F19628-95-C-0002. The opinions, interpretations, conclusions and recommendations are those of the author and are not necessarily endorsed by the United States Air Force.
†Fax: 781-981-0122; e-mail: wang@ll.mit.edu.

1. Introduction

$Ga_{1-x}In_xAs_ySb_{1-y}$ alloys are of interest for lattice-matched thermophotovoltaic (TPV) devices because of the high performance attainable at 2.3 μm [1]. Extension of the TPV device cutoff wavelength (λ_c) to beyond this wavelength is especially desirable since the emissive power of the radiator is significant at these longer wavelengths and higher power density can be attained [2]. However, the $Ga_{1-x}In_xAs_ySb_{1-y}$ quaternary alloy system exhibits a miscibility gap [3] in the wavelength range of interest. Thus, to increase λ_c requires the growth of high quality alloys that penetrate further into the miscibility gap. The growth has been difficult because these alloy compositions are metastable, and consequently, no devices with $\lambda_c > 2.3$ μm have been demonstrated previously.

In this paper, the development of $Ga_{1-x}In_xAs_ySb_{1-y}$ alloys for TPV devices with extended λ_c is reported. Epitaxial $Ga_{1-x}In_xAs_ySb_{1-y}$ layers of various composition, and thus λ_c, were grown lattice matched to GaSb substrates by organometallic vapor phase epitaxy (OMVPE). The materials properties including the structural, optical, and electrical are compared for epilayers with λ_c varying from 2 to 2.5 μm. The data indicate that the overall material quality suffers for alloys moving into the miscibility gap, i.e., with increasing x- and y-values. In spite of the degradation, the internal quantum efficiency of TPV devices is as high as 86%.

2. Epitaxial growth and characterization

$Ga_{1-x}In_xAs_ySb_{1-y}$ epilayers were grown in a vertical rotating-disk reactor with H_2 carrier gas at a flow rate of 10 slpm, reactor pressure of 150 Torr, and a typical rotation rate of 100 rpm [4]. Solution trimethylindium (TMIn), triethylgallium (TEGa), tertiarybutylarsine (TBAs), and trimethylantimony (TMSb) were used as organometallic precursors. Diethyltellurium (DETe) (10 ppm in H_2) and dimethylzinc (DMZn) (1000 ppm in H_2) were used as n- and p-type doping sources, respectively. For lattice-matched epilayers, $Ga_{1-x}In_xAs_ySb_{1-y}$ was grown without a GaSb buffer on (100) Te-doped GaSb substrates misoriented 6° toward (111)B. The growth temperature was 525°C, and the V/III ratio ranged from 1.3 to 1.7.

The surface morphology was examined using Nomarski contrast microscopy and atomic force microscopy (AFM) in the tapping mode. High-resolution axis x-ray diffraction (HRXRD) was used to measure the degree of lattice mismatch to GaSb substrates. Photoluminescence (PL)

was measured at 4 and 300 K using a PbS detector. The In and As contents of $Ga_{1-x}In_xAs_ySb_{1-y}$ epilayers were determined from the combination of 1) HRXRD splitting of ω-2Θ scans; 2) peak emission in 300 K PL spectra; and 3) energy gap dependence on composition, $E(x,y) = 0.726 - 0.961x - 0.501y + 0.08xy + 0.415x^2 + 1.2y^2 + 0.021x^2y - 0.62xy^2$, where $y = 0.867x/(1 - 0.048x)$ for alloys lattice matched to GaSb substrates. For electrical characterization, GaInAsSb was grown on SI (100) GaAs substrates. Because of the lattice mismatch between the epilayer and the substrate, a 0.4 μm-thick GaSb buffer layer was grown [4]. Carrier concentration and mobility of GaInAsSb epilayers, which were grown about 3 μm thick, were obtained from Hall measurements based on the van der Pauw method.

3. Growth results

3.1 Surface morphology

Nomarski micrographs of the surface morphology of $Ga_{1-x}In_xAs_ySb_{1-y}$ layers lattice matched to GaSb substrates are shown in Fig. 1. The In and As concentrations were varied with $0.09 < x < 0.23$ and $0.08 < y < 0.21$. As the In and As concentrations increase, the surface morphology exhibits an increased 'wavy' texture. Layers with x and y values less than approximately 0.21 had a mirror-like appearance to the eye (Fig. 1a – 1c). For $x \sim 0.23$, $y \sim 0.21$, the surface was hazy (Fig. 1d).

Figure 2 shows AFM images corresponding to the layers shown in Fig. 1. AFM images the microscopic surface features and a marked increase in surface roughness is measured as the x- and y-values increase. The root-mean-square roughness for these layers is 0.2, 0.8, 1.5, and 8 nm, respectively, for images shown in Figs. 2a – 2d. The surface features that are oriented in the [011] direction for layers shown in Fig. 2a – 2c are consistent with a step-bunching growth mode. The irregular pattern observed for the layer shown in Fig. 2d suggests a three-dimensional growth mode. The degradation in surface morphology may be related to the increased instability of the alloy since this composition corresponds to a region further inside the miscibility gap [3].

3.2 High-resolution X-ray diffraction

The HRXRD of nominally lattice matched $Ga_{1-x}In_xAs_ySb_{1-y}$ epilayers also exhibits a dependence on the In and As concentrations. Figure 3 shows ω-2Θ scans plotted on a log scale for epilayers about 2 μm in thickness. (The corresponding surface morphology is shown in Figs.

1a-1c.) For the epilayer with the lowest x and y values (x = 0.09, y = 0.08) shown in Fig. 3a, the full width at half-maximum (FWHM) of the epilayer peak is comparable to that of the GaSb substrate (23 arc s). The FWHM increases to 32 arc s with increasing In- and As-values (Fig. 3b). For x = 0.20, y = 0.18 (Fig. 3c), the epilayer is matched to the substrate, but the scan is substantially broadened. This broadening may be related to a range of d-spacings associated with early stages of phase separation of the $Ga_{1-x}In_xAs_ySb_{1-y}$ metastable alloy to GaAs- and InSb-rich regions.

3.3 Optical properties

Figure 4 shows the 4 and 300 K PL spectra for $Ga_{1-x}In_xAs_ySb_{1-y}$ epilayers discussed in the previous figures a – c. The peak emission for the sample shown in Fig. 4a with x = 0.09, y = 0.08 is 1818 and 2035 nm at 4 and 300 K, respectively. The 4 K FWHM is 5.3 meV. With increasing x and y values, the 4 and 300 K emission increases to 2080 and 2320 nm, respectively, for x = 0.16, y = 0.15 (Fig. 4b); and to 2225 and 2505 nm, respectively, for x = 0.2, y = 0.18 (Fig. 4c). The 4 K FWHM also increases to 7.5 and 25 meV, respectively. Although lattice matched $Ga_{1-x}In_xAs_ySb_{1-y}$ of higher In and As compositions (see Figs. 1d and 2d) was epitaxially grown, this layer did not exhibit PL at 4 or 300 K. The longest PL emission at 300 K observed in our current study is 2525 nm.

Figure 5 summarizes the 4 K PL FWHM data for $Ga_{1-x}In_xAs_ySb_{1-y}$ epilayers grown in this study as well as in our previous studies [4]. These layers were grown at 525, 550, and 575°C. Several trends are observed. The PL FWHM values are strongly dependent on growth temperature and peak energy. The lowest PL FWHM values are obtained for layers grown at the lowest temperature of 525°C. The narrowest PL FWHM values are ~5 meV for 4 K peak energy greater than 0.62 eV, and increase sharply below 0.60 eV. On the other hand, the PL FWHM increases below ~0.63 and 0.67 eV for layers grown at 550 and 575°C, respectively. Since broadening in PL spectra can be a result of alloy scattering [5], the data are consistent with increased alloy clustering especially for layers with composition approaching the miscibility gap. These results suggest that under nonequilibrium conditions for OMVPE growth, the kinetics can have a significant influence on the extent of penetration into the miscibility gap. The smallest FWHM value measured is 4.7 meV at 0.643 eV, which is the lowest value that has been

reported for this alloy system grown by OMVPE [3,6,7]. Our FWHM values are comparable to those reported for layers grown by molecular beam epitaxy [8] and by liquid phase epitaxy [9].

3.4 Electrical properties

The 300 K electrical properties of p- and n-doped $Ga_{1-x}In_xAs_ySb_{1-y}$ are summarized in Figs. 6a and 6b, respectively. The plots include data for layers grown at 525 and 550°C on (100) 2° toward (110) and (100) 6° toward (111)B substrates. The majority of the data that are shown as the filled circles corresponds to layers with 300 K PL emission at ~2.2 μm. The hole concentration ranges from 4.4 x 10^{15} to 1.9 x 10^{18} cm^{-3} with mobility values between 560 and 180 cm^2/V-s, respectively. The two higher mobility values measured for p-GaInAsSb at the lower concentration ~8 x 10^{15} cm^{-3} are data for samples with a 0.8-μm-thick GaSb buffer layer. A dependence of the p-type electrical characteristics on the alloy composition is measured, with lower mobility values obtained as the x- and y-values increase. The electron concentration ranges from 2.2 x 10^{17} to 3.2 x 10^{18} cm^{-3}, with corresponding mobility values between 5208 and 2084 cm^2/V-s, respectively. However, the data suggest that the electrical characteristics of the n-doped GaInAsSb are independent of alloy composition.

4. Thermophotovoltaic Devices

TPV device structures were grown on (100) 6° toward (111)B GaSb substrates. The growth temperature was 525°C. The TPV structure consists of the following layers: 0.1-μm-thick n-GaSb buffer layer, 1-μm-thick n-GaInAsSb base layer (doped to 5 x 10^{17} cm^{-3}), 4-μm-thick p-GaInAsSb emitter layer (doped to 2 x 10^{17} cm^{-3}), and 0.05-μm-thick p-GaSb contact layer (doped to 2 x 10^{18} cm^{-3}), grown on a GaSb substrate. Thick emitter layers were incorporated to take advantage of the longer minority carrier diffusion lengths in the p-type layer [10]. The composition of the GaInAsSb alloy was varied to obtain various λ_c.

Large-area (1 cm^2) TPV cells were fabricated by a conventional photolithographic process. A single 1-mm-wide central busbar connected to 10-μm-wide grid lines spaced 100 μm apart was used to make electrical contact to the front surface. Ohmic contacts to p- and n-GaSb were formed by depositing Ti/Pt/Au and Au/Sn/Ti/Pt/Au, respectively, and alloying at 300°C.

Mesas were formed by wet chemical etching to a depth of ~5 μm. No antireflection coatings were deposited on these test devices.

The external quantum efficiency (QE) of three TPV devices with various λ_c is plotted as a function of wavelength in Fig. 7. A maximum QE is measured at ~2 μm, and is 59, 58, and 57%, respectively for devices with λ_c of 2.3, 2.4, and 2.5 μm. The QE decreases below 1.6 μm because of absorption in the GaSb window layer. The internal QE exceeds 85% in all cases based on a surface reflection of 34%.

Figure 8 shows the open circuit voltage (V_{oc}) as a function of short circuit current density (J_{sc}) for a typical device with λ_c of 2.3 μm measured at 25°C. At 1 A/cm^2, V_{oc} is 290 meV. This value is slightly lower than the value of 300 meV reported for TPV structures with a 3 μm-thick emitter layer [1,8]. This reduction is a result of the increased dark current for TPV devices with thicker emitter layers. The best V_{oc} values for lattice-mismatched InGaAs/InP TPV devices are similar even though those devices had a shorter cutoff wavelength of 2.2 μm [11], thus showing the advantage of lattice-matched GaInAsSb/GaSb TPV structures. The fill factor for the GaInAsSb/GaSb devices is typically 69%.

5. Summary

High quality metastable $Ga_{1-x}In_xAs_ySb_{1-y}$ epilayers were grown lattice matched to GaSb substrates by OMVPE using TEGa, TMIn, TBAs, and TMSb. Room temperature PL emission at wavelengths as long as 2.5 μm was achieved by using a low growth temperature of 525°C. Low temperature photoluminescence (PL) spectra exhibit FWHM as narrow as ~5 meV, which is the smallest value reported for GaInAsSb alloys grown by OMVPE. An increase in surface roughness and broadening in FWHM of 4K PL spectra and HRXRD are observed for epilayers with increasing x- and y-values. The external QE of TPV devices is as high as 57 to 59 % for with λ_c between 2.3 and 2.5 μm.

Acknowledgments

The authors gratefully acknowledge D.R. Calawa for x-ray diffraction, J.W. Chludzinski for photoluminescence, K.J. Challberg for manuscript editing, and D.L. Spears for continued support and encouragement.

References

1. H.K. Choi, C.A. Wang, G.W. Turner, M.J. Manfra, D.L. Spears, G.W. Charache, L.R. Danielson, and D.M. Depoy, Appl. Phys. Lett. 71 (1997) 3758.

2. P.F. Baldasaro, E.J. Brown, D.M. Depoy, B.C. Campbell, and J.R. Parrington, 1st NREL Conference on the Thermophotovoltaic Generation of Electricity, edited by T.J. Coutts and J.P. Benner, AIP Conference Proceedings Vol. 321, Woodbury, NY, 1995.

3. M.J. Cherng, H.R. Jen, C.A. Larsen, G.B. Stringfellow, H. Lundt, and P.C. Taylor, J. Cryst. Growth 77 (1986) 408.

4. C.A. Wang, accepted J. Cryst. Growth.

5. J. Singh and K.K. Bajaj, Appl. Phys. Lett. 44 (1984) 1075.

6. J. Shin, T.C. Hsu, Y. Hsu, and G.B. Stringfellow, J. Cryst. Growth 179 (1997) 1.

7. M. Sopanen, T. Koljonen, H. Lipsanen, and T. Tuomi, J. Cryst. Growth 145 (1994) 492.

8. C.A. Wang, H.K. Choi, G.W. Turner, D.L. Spears, M.J. Manfra, and G.W. Charache, in 3rd NREL Conference on the Thermophotovoltaic Generation of Electricity, edited by J.P. Benner and T.J. Coutts, AIP Conference Proceedings Vol. 401, Woodbury, NY, 1997, p. 75.

9. E. Tournie, J.-L. Lazzari, F. Pitard, C. Alibert, A. Joullie, and B. Lambert, J. Appl. Phys. 68 (1990) 5936.

10. C.W. Hitchcock, R.J. Gutmann, H. Ehsani, I.B. Bhat, C.A. Wang, M.J. Freeman, and G.W. Charache, presented at ICMOVPE IX, 1998.

11. G.W. Charache, J.L. Egley, L.R. Danielson, D.M. DePoy, P.F. Baldasaro, B.C. Campbell, S. Hui, L.M. Frass, and S. Wojtczuk, Proc. 25th IEEE Photovoltaic Specialist Conf. (1996) 137.

Figure Captions

Figure 1 Surface morphology of nominally lattice matched $Ga_{1-x}In_xAs_ySb_{1-y}$ epilayers grown at 525°C on (100) 6° toward (111)B GaSb substrates with compositions: (a) x = 0.09, y = 0.08; (b) x = 0.16, y = 0.15; (c) x = 0.20, y = 0.18; (d) x ~ 0.23, y ~ 0.21 The composition for the layer shown in (d) is estimated from the In distribution coefficient [4] since no room temperature photoluminescence was observed from the epilayer.

Figure 2 Atomic force microscopy images of epilayers shown in Figure 1. Alloy compositions (a) x = 0.09, y = 0.08; (b) x = 0.16, y = 0.15; (c) x = 0.20, y = 0.18; (d) x ~ 0.23, y ~ 0.21. Note the change in vertical scale for (d).

Figure 3 High resolution x-ray diffraction of $Ga_{1-x}In_xAs_ySb_{1-y}$ epilayers grown at 525°C on (100) 6° toward (111)B GaSb substrates with compositions: (a) x = 0.09, y = 0.08; (b) x = 0.16, y = 0.15; (c) x = 0.20, y = 0.18.

Figure 4 Photoluminescence spectra measured at 4 and 300 K of $Ga_{1-x}In_xAs_ySb_{1-y}$ grown on (100) 6° toward (111)B GaSb substrates. Layers were grown at 525°C: (a) x = 0.09, y = 0.08; (b) x = 0.16, y = 0.15; (c) x = 0.20, y = 0.18.

Figure 5 Photoluminescence full width at half-maximum measured at 4 K of GaInAsSb layers grown on GaSb substrates at 525°C (open squares), 550°C (solid circles), and 575°C (open circles). Dashed lines provided only to guide the eye.

Figure 6 Electrical properties measured at 300 K of (a) p-GaInAsSb and (b) n-GaInAsSb.

Figure 7 External quantum efficiency of GaInAsSb /GaSb TPV devices as a function of wavelength. Emitter layer thickness is 4 μm.

Figure 8 Open circuit voltage as a function of short circuit current density for GaInAsSb /GaSb TPV device with cutoff wavelength of 2.3 μm.

315624-2P

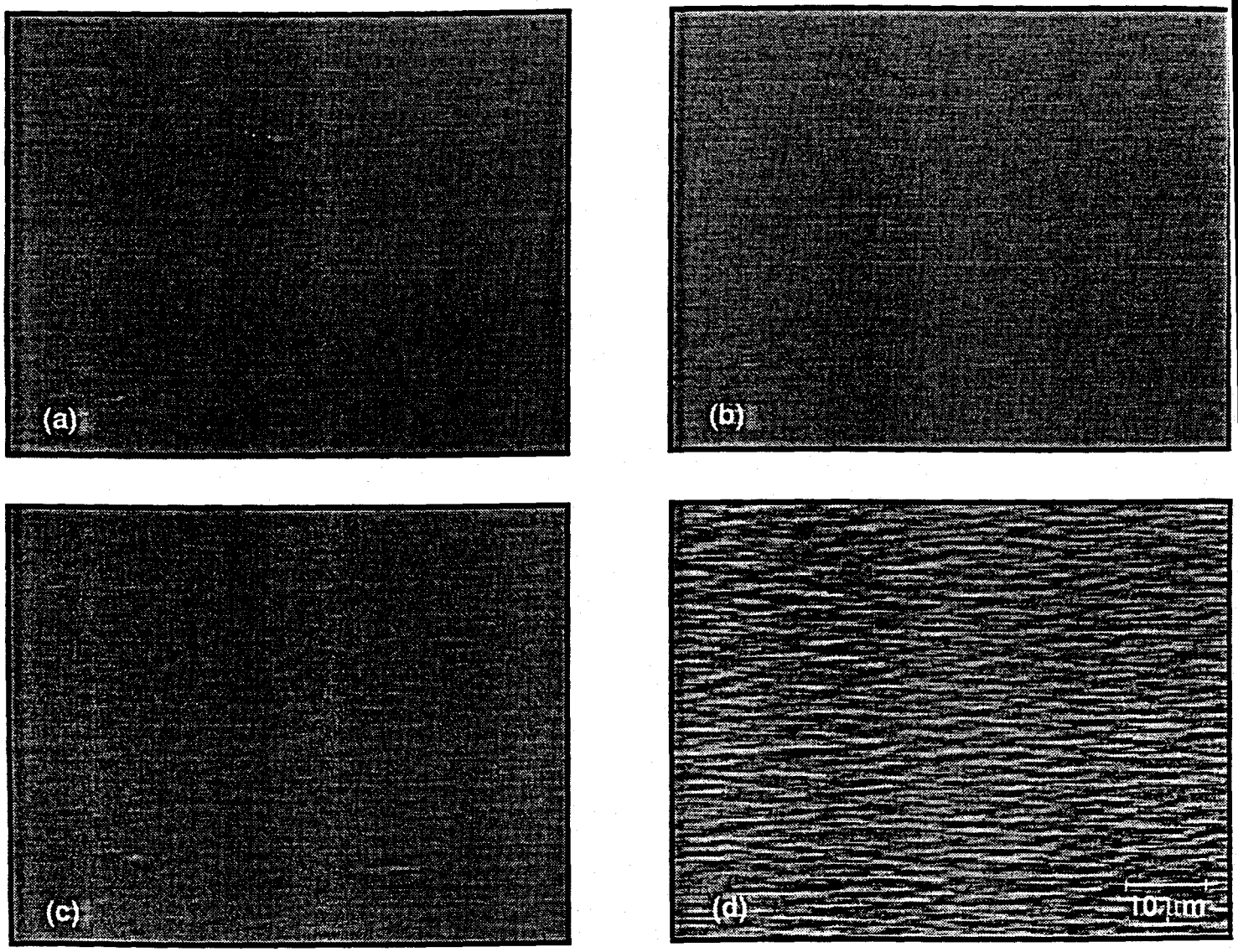

Figure 1

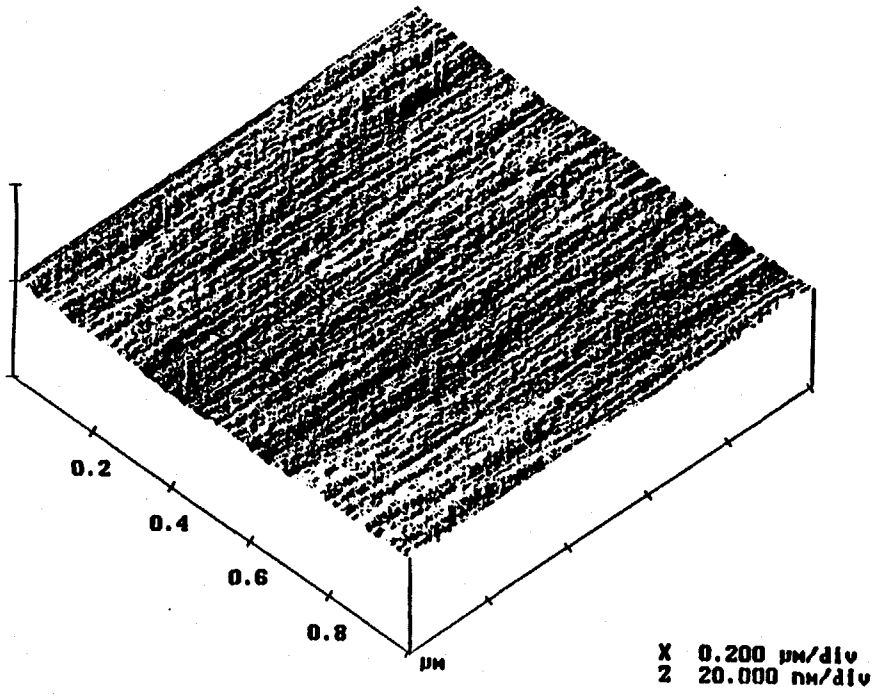
0.2
0.4
0.6
0.8
μm
X 0.200 μm/div
Z 20.000 nm/div

(a)

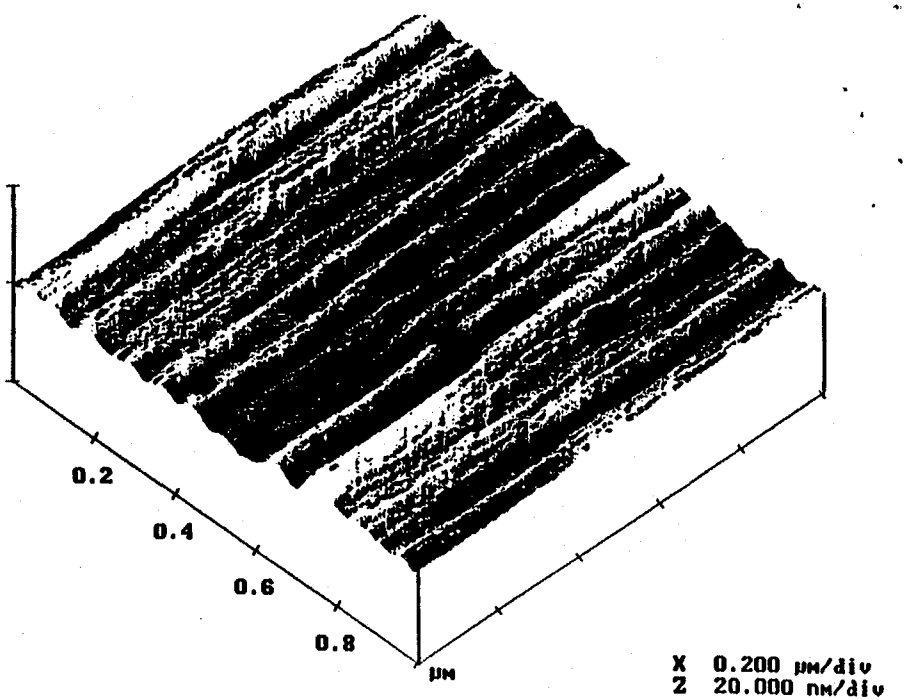
0.2
0.4
0.6
0.8
μm
X 0.200 μm/div
Z 20.000 nm/div

(b)

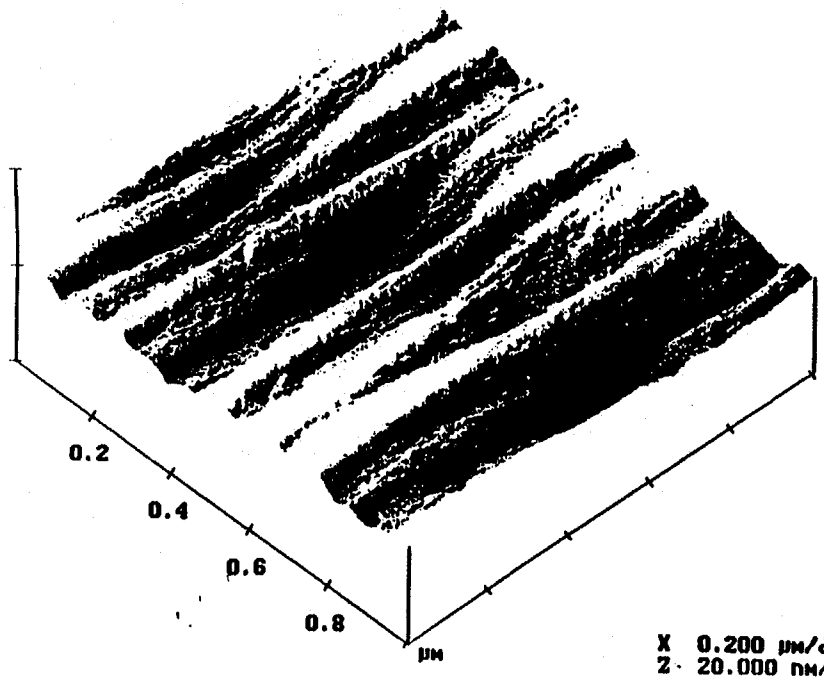
0.2
0.4
0.6
0.8
μm
X 0.200 μm/div
Z 20.000 nm/div

(c)

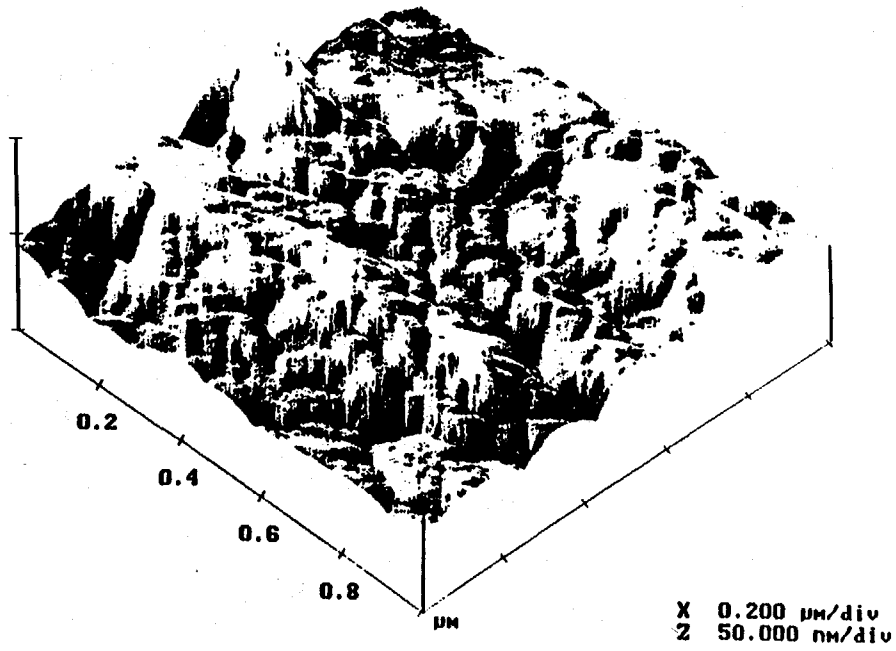
0.2
0.4
0.6
0.8
μm
X 0.200 μm/div
Z 50.000 nm/div

(d)

315624-3

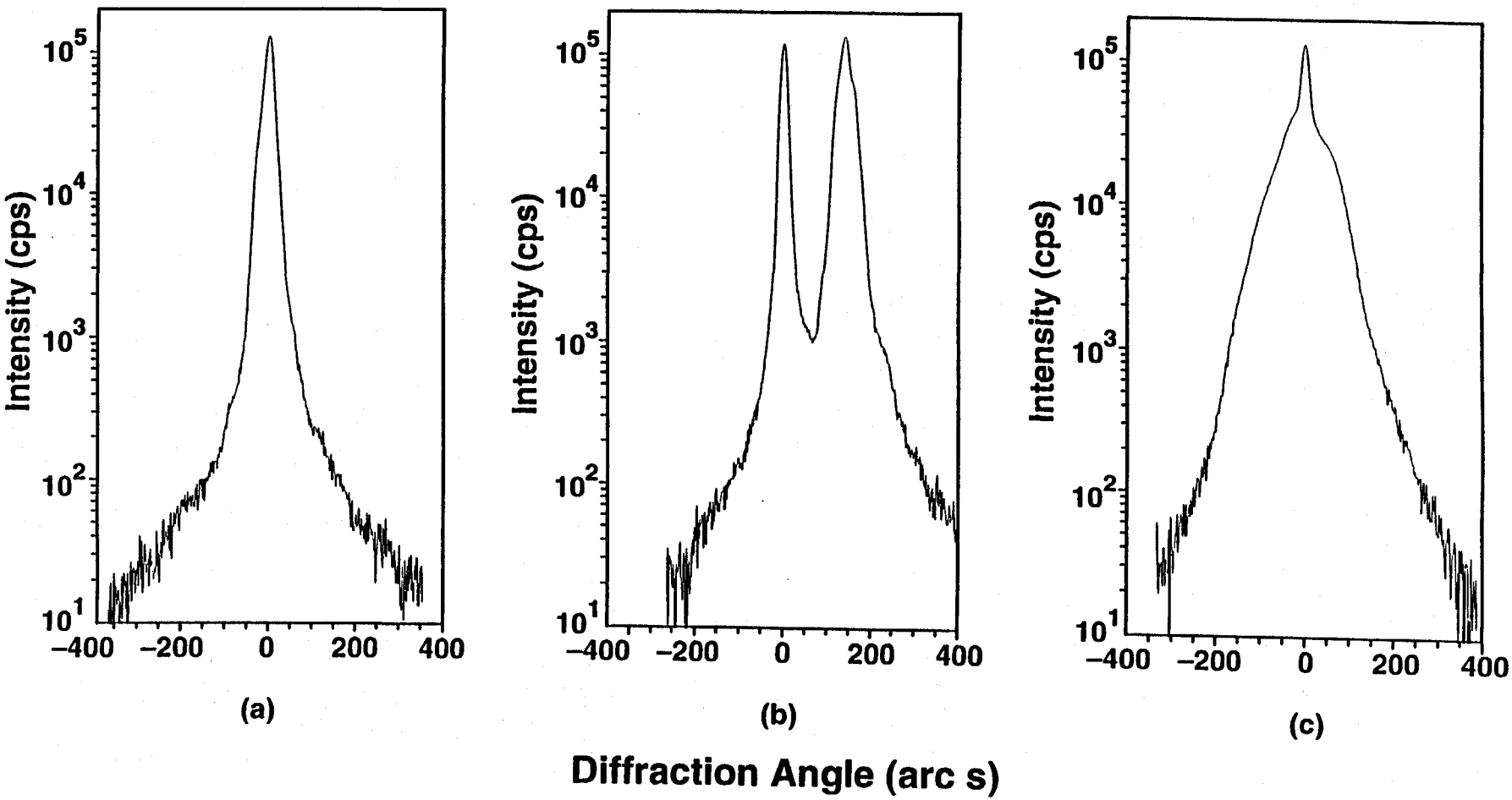

Figure 3

315624-4

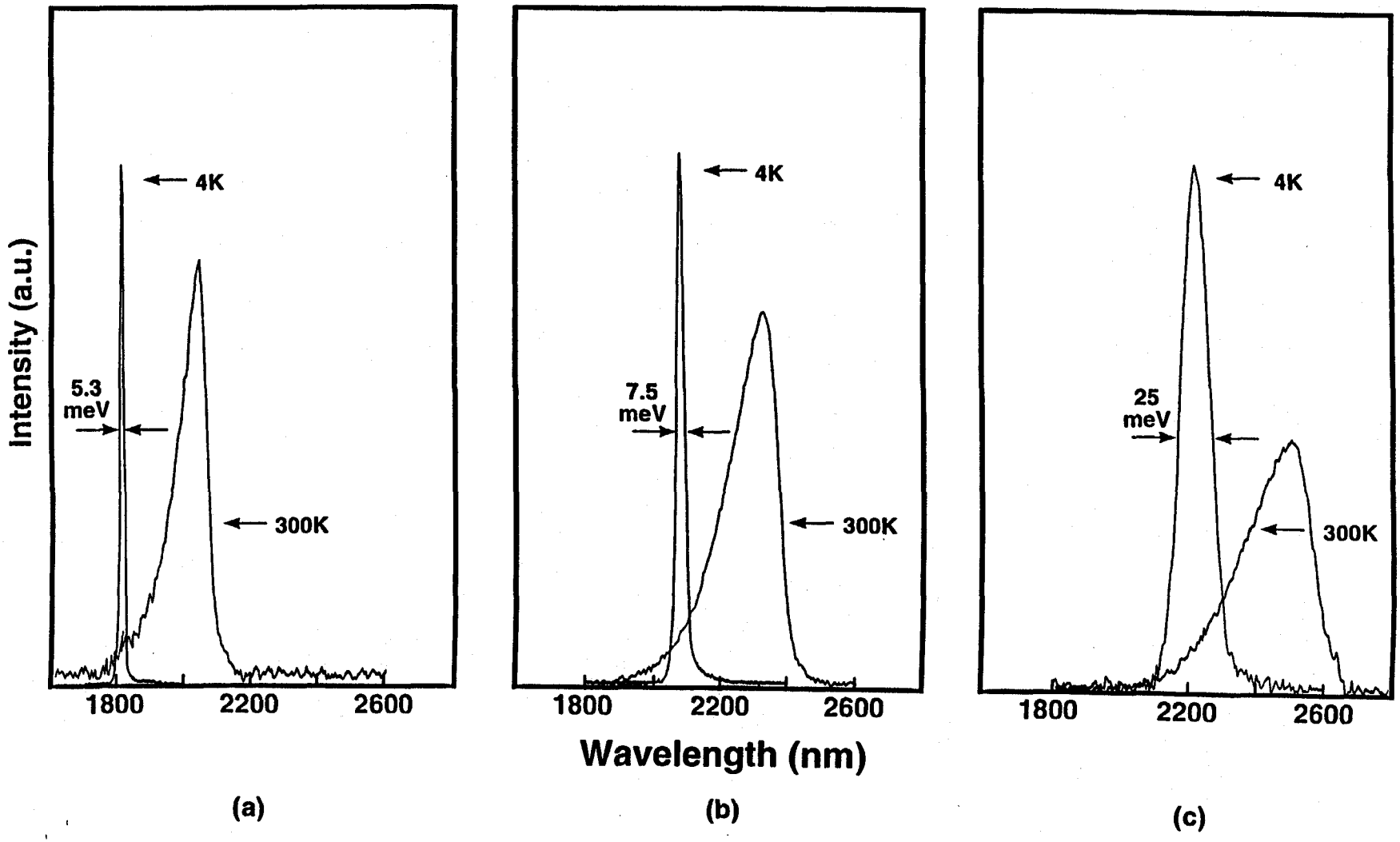

Figure 4

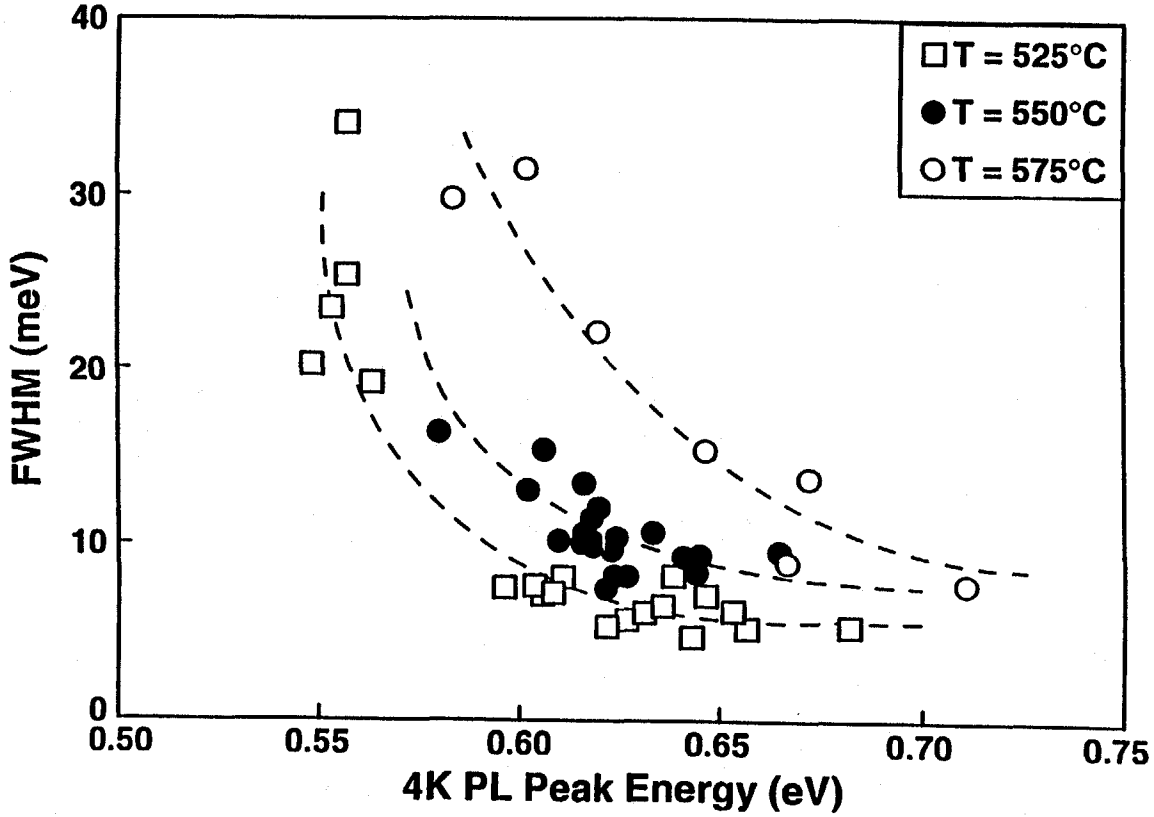
T = 525°C
T = 550°C
T = 575°C
FWHM (meV)
40
30
20
10
0
0.50
0.55
0.60
0.65
0.70
0.75
4K PL Peak Energy (eV)

Figure 5

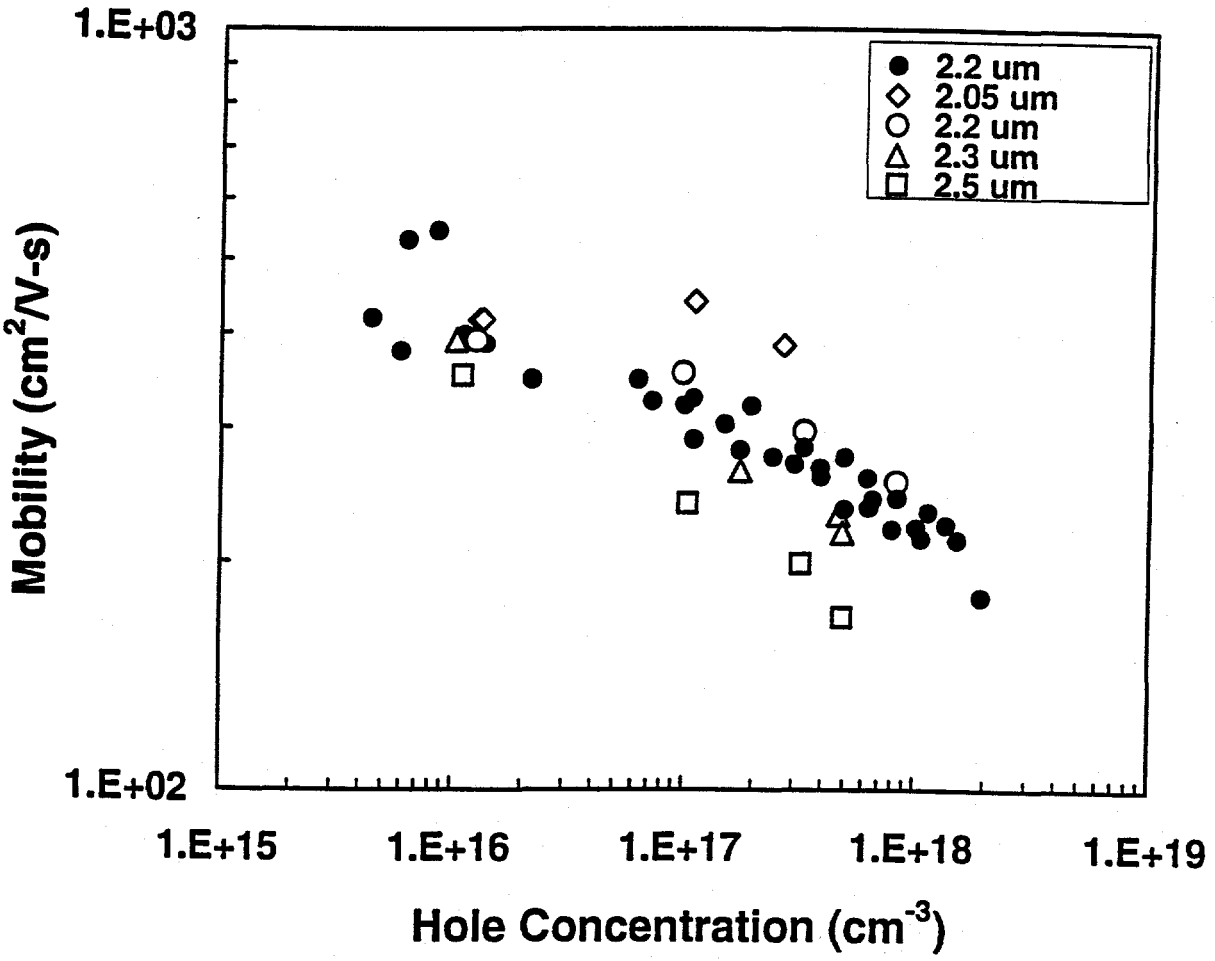
1.E+03
1.E+02
Mobility (cm²/V-s)
2.2 um
2.05 um
2.2 um
2.3 um
2.5 um
1.E+15
1.E+16
1.E+17
1.E+18
1.E+19
Hole Concentration (cm⁻³)

Figure 6a

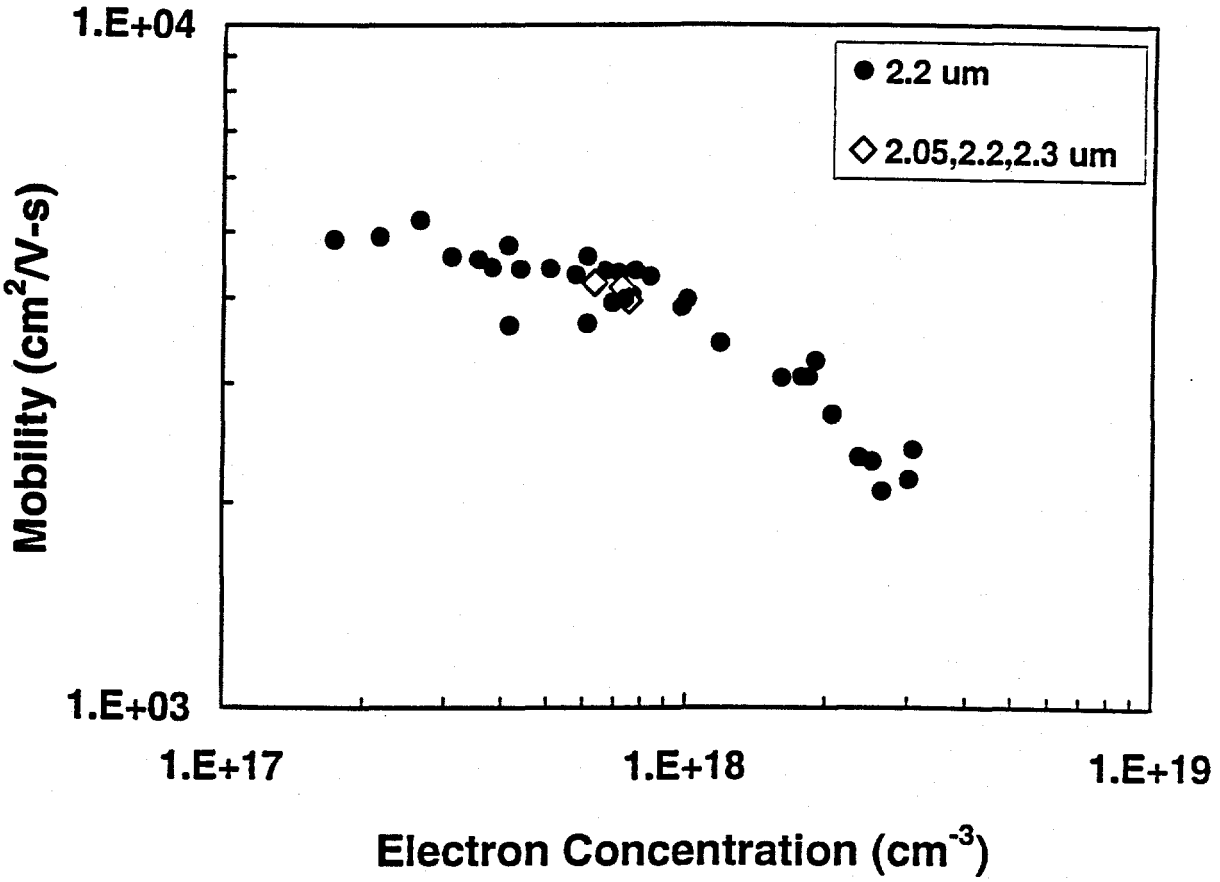
1.E+04
1.E+03
1.E+17
1.E+18
1.E+19
Mobility (cm²/V-s)
Electron Concentration (cm⁻³)
2.2 um
2.05,2.2,2.3 um

Figure 6b

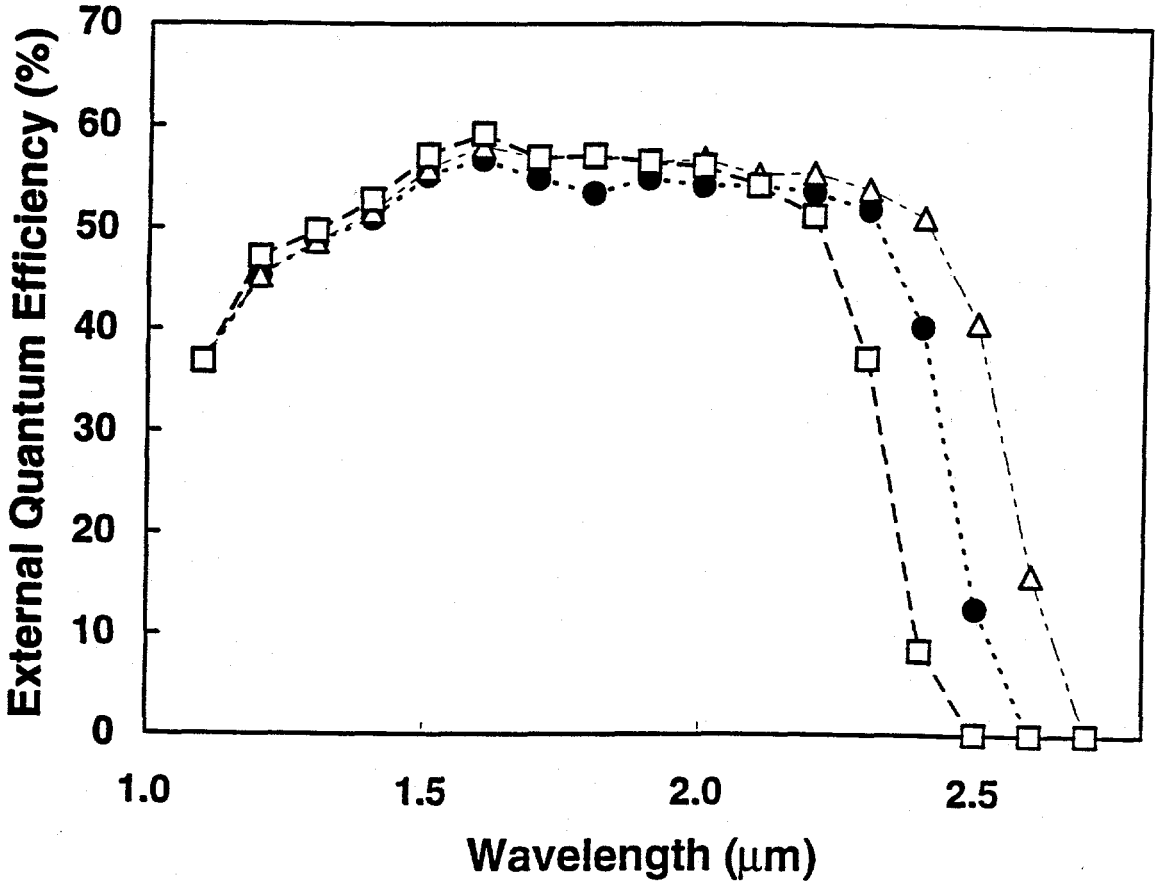
External Quantum Efficiency (%)
70
60
50
40
30
20
10
0
1.0
1.5
2.0
2.5
Wavelength (μm)

Figure 7

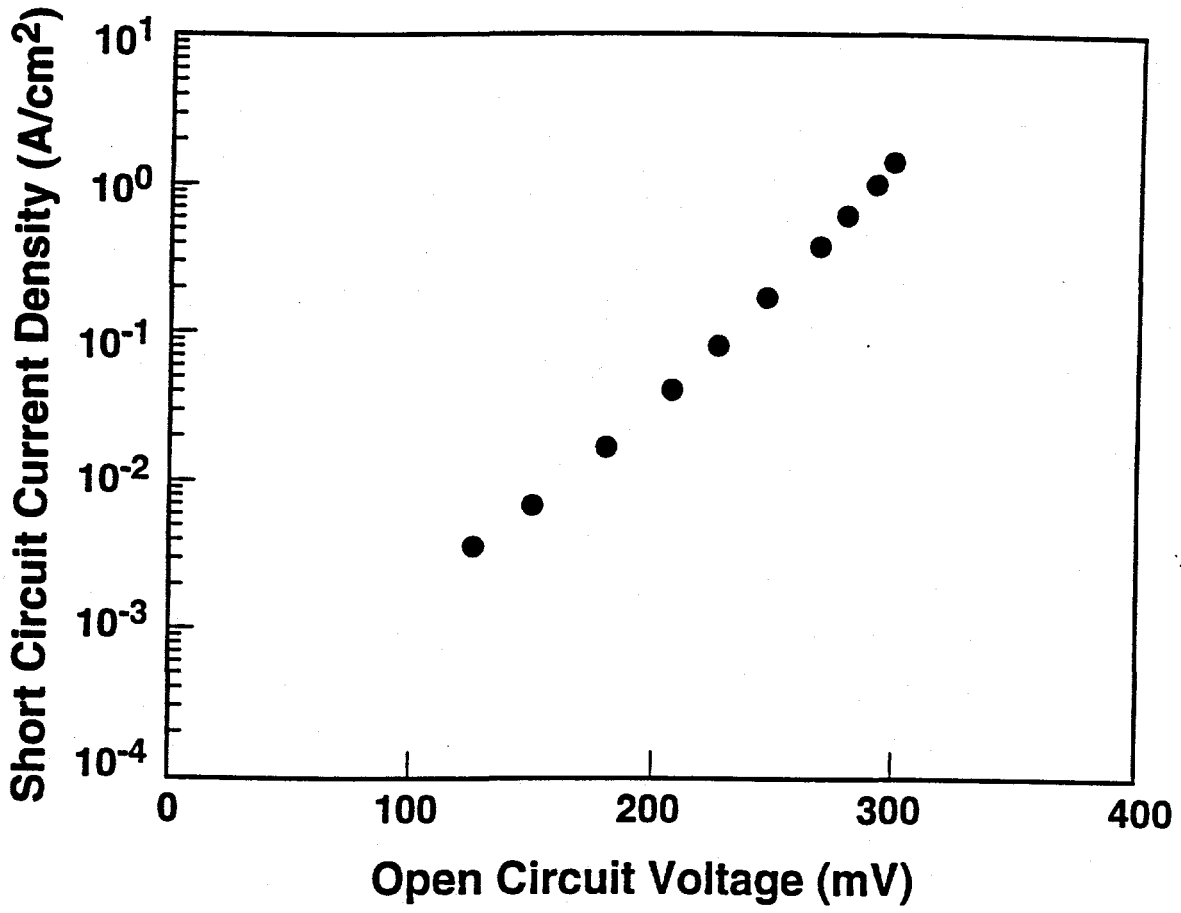
Short Circuit Current Density (A/cm²)
10¹
10⁰
10⁻¹
10⁻²
10⁻³
10⁻⁴
0
100
200
300
400
Open Circuit Voltage (mV)
316383-1

Figure 8